Available online at www.sciencedirect.com
ScienceDirect
Dyes and Pigments 74 (2007) 161–168
DYES and PIGMENTS
www.elsevier.com/locate/dyepig

The preparation of magnetite, goethite, hematite and maghemite of pigment quality from mill scale iron waste

M.A. Legodi, D. de Waal*

Department of Chemistry, University of Pretoria, 0002 Pretoria, South Africa

Received 4 November 2005; accepted 23 January 2006
Available online 17 April 2006

Abstract

Mill scale iron waste has been used to prepare some iron oxide pigments via specific precursors. Magnetite and goethite were precipitated from their respective precursors in aqueous media. Various red shades of hematite were prepared by the calcinations of the precipitated goethite at temperatures ranging from 600 to 900 °C. Maghemite was obtained by thermal treatment of magnetite at 200 °C. The iron oxides were characterized by Raman spectroscopy, X-ray diffraction (XRD), surface area determination and scanning electron microscopy (SEM). They are generally composed of very small particles (mainly <0.1 μm) with high surface area. These particle properties suggest that the above pigments (prepared from mill scale) will show high tinting strength, quality hiding power and good oil absorption. Oil absorption is a property of the pigment that is closely related to the ease of dispersion.
© 2006 Elsevier Ltd. All rights reserved.

Keywords: Mill scale; Raman; Iron oxides; Pigments; Precipitation

1. Introduction

Stainless steel finishing operations involve several cleaning processes, which eliminate dust, scale and metallic oxides [1]. Mill scale is a steel making by-product from steel hot rolling processes and is basically composed of iron oxides and metallic iron with variable oil and grease contents [2,3]. Its specific production is about 35–40 kg/t of hot rolled product [2]. The oil component in rolling mill scale makes the recycling difficult, and its direct re-use in sintering may lead to environmental pollution. Mill scale with high oil content is recycled after extracting the oil in a pretreatment stage. Coarse scale with a particle size of 0.5–5 mm and oil content of less than 1% can be returned to the sinter strand without any pretreatment. High oil content (>3%) results in increased emission of volatile organic compounds including dioxins and can lead to problems in waste gas purification systems, e.g. glow fires in electrostatic precipitators. Because of this mill scale needs to be pretreated before it can be re-used. Fine sludge mainly consists of very small-scale particles (0.1 mm). Since the fine particles adsorb oil to a very high degree (5–20%) this scale normally cannot be returned to the sinter strand without pretreatment [4]. The oil adsorption in the preceding line refers to the metallic mill scale and should not be confused with the oil absorption, pigment property, mentioned in the abstract and elsewhere in this paper. At MITTAL (former ISCOR), a steel manufacturing company in the Republic of South Africa, the bulk of mill scale waste is dumped in landfills. The continuous demand for more landfills and the leaching of some small percentages of heavy metals into soil and ground water, thus threatening the environment, highlight the need for more effective methods of waste disposal and productive utilisation of mill scale.

Production of iron oxide pigments is one of the possible ways of alleviating the problem facing the steel industry in RSA since mill scale has a high iron content in the form of oxides and metal. The use of iron waste in iron oxide preparations is vital because of the increasing demand for iron

* Corresponding author. Tel.: +27 1 242 030 99; fax: +27 123 625 297.
E-mail address: danita.dewaal@up.ac.za (D. de Waal).

0143-7208/$ - see front matter © 2006 Elsevier Ltd. All rights reserved.
doi:10.1016/j.dyepig.2006.01.038

oxide pigments driven by the increases in construction activities, current economic needs [5] in emerging markets and growing concern over the use of heavy metal-based pigments. The increasing importance of iron oxide pigments is also based on their non-toxicity, chemical stability, durability [6], wide variety of colours and low costs.

There are many studies in the literature that deal with different methods for the preparation of magnetite [7–11], hematite [12–15], maghemite [16–20] and goethite [21–23]. These are the iron oxides commonly used as pigments giving black, red, brown and yellow colours, respectively. Steel pickling chemical waste (SPW) has been thermally decomposed at various temperatures to give red iron oxide (hematite) [9,24,25]. The formation of mill scale (mainly FeO and Fe) can also be accompanied by the precipitation of corrosion product mixture, viz. Fe_3O_4, FeOOH, Fe_2O_3, etc. [26]. FeO is usually closest to the metal surface while Fe_2O_3 forms the outer layer [27]. Since corrosion products occur in a mixture and the overall mill scale is hardened and of poor colour, it is not of pigment value. Oulsnam and Erasmus [28] have succeeded in preparing magnetite from ferrous mill scale using a dry oxidation step. However, the particles of their product were too large and had to be ground (wet and dry) to <10 μm to improve the pigment qualities (colour, tinting strength, hiding power and oil absorption) [24,25]. Hematite was prepared by calcination of the obtained magnetite and its particles also had to be ground to sizes < 10 μm.

The present study was undertaken with the aim of preparing magnetite and goethite of pigment particle size < 10 μm via water-soluble mill scale-derived precursors. Furthermore, maghemite and hematite could then be prepared by thermal treatment of the obtained magnetite and goethite, respectively.

2. Experimental

2.1. Chemical preparation

2.1.1. Ferrous precursor

Conc. H_2SO_4 (analytical reagent, 300 ml) was added to 60 g of raw mill scale in a 600 ml glass beaker. The mixture when heated on a hot plate became turbid. The turbid mixture was further heated to dryness. The resulting muddy solid product was then used as the starting material for the preparation of magnetite and goethite. Preliminary investigations showed that the product was soluble in water (more readily in warm water) and a dark blue/green flaky sediment resulted when the aqueous solution was mixed with a base (e.g. NH_4OH or NaOH). This chemical behaviour is characteristic of the presence of $Fe(OH)_2$ in solution [21]. It indicates that the greater part of iron in the muddy solid product is in the Fe^{2+} form. The acidic environment was created in order to facilitate the conversion of iron oxides to ferrous or ferric ions in an aqueous solution [29].

2.1.2. Ferric precursor

Conc. H_2SO_4 (300 ml) was mixed with 30 g of raw mill scale in a 600 ml glass beaker. The mixture was then heated to dryness on a hot plate. The product, containing a fine white powder and dark solid particles, was cooled to room temperature and allowed to stand in open air for five days. During this time the product gradually turned into a yellowish fine white powder. No darker areas were observed. The fine powder was soluble in warm water and formed rust coloured sediment when a base, e.g. NH_4OH or NaOH, was added to its aqueous solution. This chemical behaviour is characteristic of the presence of $Fe(OH)_3$ [21]. Therefore, the greater part of iron in the fine yellowish white powder was in the form of Fe^{3+} [29].

Alternatively, 60 g of mill scale in 200 ml of conc. H_2SO_4 was digested on a hot plate at 100 °C for 30 min followed by the addition of 200 ml of 65% HNO_3. Further heating resulted in a cream white homogeneous solid substance, which was then heated to dryness. The cream white solid contained iron mainly in the Fe^{3+} form.

2.1.3. Magnetite (Fe_3O_4)

Magnetite was prepared by the method of Ueda et al. [8] with some modifications. Ferrous precursor (10 g) was dissolved in 120 ml of distilled water. To the filtered solution 130 ml of 25% NH_4OH solution was added, thus raising the pH to about 11–12. After ageing at room temperature for 20 h, the precipitate formed was collected by filtering. The precipitate was washed with 500 ml of distilled water and allowed to dry at room temperature. The black, magnetite product was qualitatively examined by Raman spectroscopy and confirmed by X-ray powder diffraction (XRD).

2.1.4. Maghemite (γ-Fe_2O_3)

The magnetite obtained above (Section 2.1.3) was heated in an oven at 200 °C for 3 h during which it turned light brown [30]. This product was identified by Raman spectroscopy and confirmed by XRD results to be maghemite.

2.1.5. Goethite (α-FeOOH)

This iron oxide polymorph was prepared using the method of Thiebeau et al. [23] with some modifications. Ferric precursor (20 g) was dissolved in 500 ml of distilled water. To the filtered solution 100 ml of 1 M $NaHCO_3$ solution was added which brought the pH to values between 5 and 7. The solution was held at 100 °C for 1 h and allowed to cool to room temperature. The resulting yellow precipitate was filtered off and washed with 300 ml of distilled water and allowed to dry in air. The product was identified by Raman spectroscopy and confirmed by XRD as goethite.

2.1.6. Hematite (α-Fe_2O_3)

The goethite obtained above, in Section 2.1.5, was calcined in the furnace at temperatures between 600 and 900 °C for 5 h. The colour of the resulting products gave the following shades of red as the temperature increased: orange-brown, brown-red, bright-red, maroon, purple and gray. The phase determination was carried out using Raman spectroscopy and XRD showed that the product was hematite.

The product particle characteristics (namely sizes, shapes and specific surface areas) were determined using scanning

electron microscopy (SEM) and BET single point surface area measurement.

2.2. Instruments

2.2.1. Raman spectroscopy

Laser Raman spectra were recorded at room temperature using a Dilor XY Raman spectrometer with a resolution of 2 cm^{-1}. Radiation at 514.5 nm from an Ar^{+} Coherent Innova 300 laser was used to excite the samples. The laser power was set at 100 mW at the source. The recording time was set between 30 and 180 s, with two accumulations per spectrum segment. An Olympus Mplan 100× objective on an Olympus BH-2 microscope was used to focus on the sample. The Raman spectra were analysed using Labspec v 2.04 software [31].

2.2.2. X-ray powder diffraction

The X-ray diffraction (XRD) analyses were performed using a Cu Kα (1.5418 Å) source (40 kV, 40 mA) from Siemens D-501, with a graphite secondary monochromator and a scintillation counter detector. The powdered sample was placed on a flat plastic plate, which was rotated at 30 rpm. The scans were performed at 25 °C in steps of 0.04°, with a recording time of 2 s for each step [32]. Where accurate 2θ values were required, Si was added as an internal 2θ standard.

2.2.3. X-ray fluorescence

An ARL 9400XP+ wavelength-dispersive XRF spectrometer with an Rh source was used for the X-ray fluorescence analyses of the samples. The XRF spectrometer was calibrated with certified reference materials. An NBSGSC fundamental parameter program was used for matrix correction of major elements, as well as Cl, Co, Cr, V, Sc and S. The Rh Compton peak ratio method was used for the other trace elements. Samples were dried and fired at 1000 °C to determine the percentage loss on ignition; for the samples this was less than 2%.

Table 1
XRF results of raw mill scale

Component	%Content
SiO_2	0.99
Al_2O_3	0.22
Fe as Fe_2O_3	103
MnO	0.800
MgO	640 ppm
CaO	660 ppm
P_2O_5	310 ppm
SO_3	0.25
Cl	260 ppm
Cr_2O_3	0.14
NiO	900 ppm
CuO	0.13
ZnO	130 ppm
ZrO_2	25 ppm
MnO_3	440 ppm
LOI	−6.3

The negative sign of the loss on ignition (LOI) value indicates that there were no volatiles in the sample.

Table 2
XRF results of ferrous and ferric mill scale precursors of iron oxides

Component	Ferrous mill scale (%)	Ferric mill scale (%)
SiO_2	0.12	2.47
Al_2O_3	0.11	2.20
Fe_2O_3	60.86	58.42
MnO	0.49	0.41
MgO	<0.01	0.64
CaO	0.08	0.09
P_2O_5	<0.01	<0.01
SO_3	38.33	35.35
Cl	<0.01	<0.01
Cr_2O_3	0.11	0.10
NiO	0.04	0.10
CuO	0.08	0.08
ZnO	0.03	<0.01
ZrO_2	<0.01	<0.01
MnO_3	<0.01	<0.01
LOI	58.34	58.85

Major element analyses were carried out on fused beads, following the standard method used in the XRD and XRF laboratory of the University of Pretoria [33], as adapted from Bennett and Oliver [34]. A pre-fired sample of 1 and 6 g of lithium tetraborate flux was mixed in a 5% Au/Pt crucible and fused at 1000 °C in a muffle furnace, with occasional swirling. The glass disk was transferred into a preheated Pt/Au mould and the bottom surface was analysed. The trace element analyses were done on pressed powder pellets, using an adaptation of the method described by Watson [35], with a saturated Mowiol 40–88 solution as binder.

2.2.4. Specific surface area (S_{BET}) determinations

Approximately 0.5 g of each sample was put into the sample container of the BET Single Point Surface Area instrument. Each sample was baked out for 30 min at 150 °C in a He/N_2 stream. The sample mass was determined after the drying process. The surface areas were determined using the standard single-point method. Samples were analysed in triplicate.

2.2.5. Scanning electron microscope (SEM)

The size and shape of the particles of iron oxide prepared in this study were monitored by the ISM 600F scanning electron microscope. Before observations, the powders were dispersed

Table 3
XRD phase results of ferrous precursor, ferric precursor, magnetite, goethite, hematite and maghemite

Sample	Phase
Ferrous mill scale	$FeSO_4 \cdot 2H_2O$, α-FeOOH, $3Fe_2O_3 \cdot 8SO_3 \cdot 2H_2O$, $FeOHSO_4$
Ferric mill scale	$FeSO_4 \cdot 2H_2O$, α-FeOOH, $3Fe_2O_3 \cdot 8SO_3 \cdot 2H_2O$, $FeOHSO_4$
Magnetite	$Fe_{2.894}O_4$
Goethite	α-FeOOH
Maghemite	γ-Fe_2O_3
Hematite	Fe_2O_3

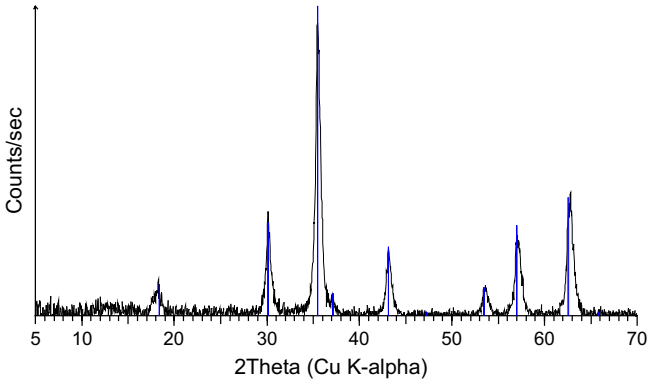

Fig. 1. X-ray powder diffractogram of magnetite obtained from mill scale.

in ethanol (100%) by ultrasonic waves. A drop of the dispersed sample was placed on a copper grid previously covered by a polymer film.

3. Results and discussion

3.1. Ferrous and ferric precursor

Tables 1 and 2 give the elemental compositions of ferrous and ferric mill scale as obtained from XRF analysis. The elemental compositions show that the percentage of iron increased significantly while the amounts of other elements decreased. This means that the acid digestion of raw mill scale increases the content of iron in the products formed. The high loss on ignition (LOI) value (over 50%) may be due to the high sulphate content, which was given off as SO_2 during the calcination that accompanied the elemental determinations.

The XRD analysis (Table 3) of both ferrous and ferric mill scale gave similar phases. The chemical behaviour of both the samples in aqueous medium shows that the ferrous mill scale contains more of ferrous compound ($FeSO_4 \cdot H_2O$) and less of ferric compounds ($3Fe_2O_3 \cdot 8SO_3 \cdot 2H_2O$, $FeOHSO_4$ and α-FeOOH) while ferric mill scale contained more of ferric

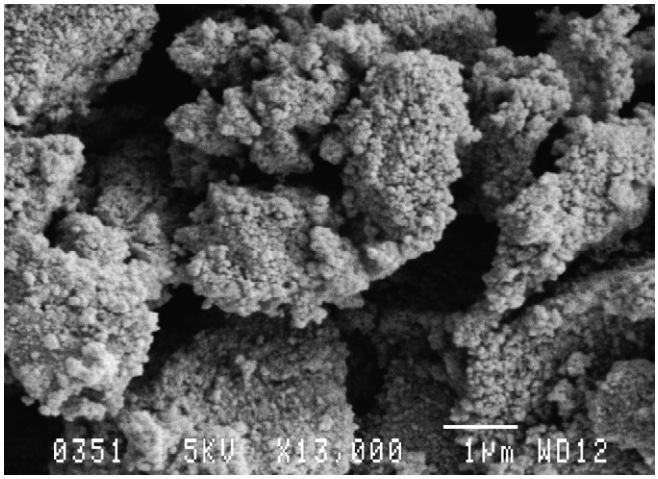

Fig. 2. SEM micrograph of magnetite obtained from mill scale.

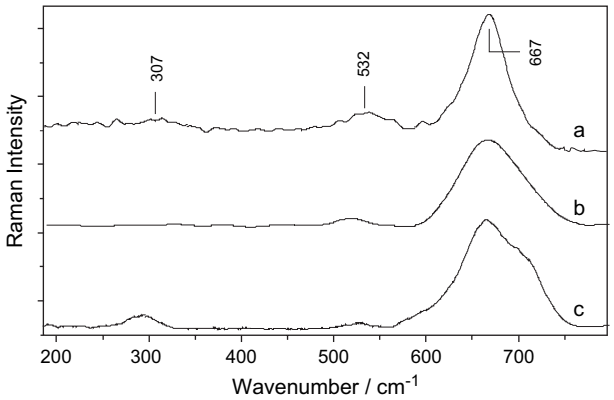

Fig. 3. Raman spectra of magnetite from various sources: (a) commercial magnetite; (b) magnetite from pure starting material and (c) magnetite obtained from mill scale.

compounds ($3Fe_2O_3 \cdot 8SO_3 \cdot 2H_2O$, $FeOHSO_4$ and α-FeOOH) and less of ferrous compounds ($FeSO_4 \cdot H_2O$).

3.2. Magnetite

The XRD analysis of the product showed largely the presence of magnetite phase. The slight broadening of the XRD lines (Fig. 1) can be interpreted in terms of poor crystallinity of the precipitated magnetite and small size of crystallites [36]. In fact the stoichiometry of this product as determined using XRD technique was $Fe_{2.894}O_4$. This suggests that the crystal structure is slightly distorted (leading to broadened XRD lines) due to the deficiency of Fe ions. The stoichiometry of magnetite with good black pigment quality should be as

Table 4
Raman wavenumbers and assignments of the prepared iron oxides

Compound	Experimental (cm^{-1})	Pure oxide (cm^{-1})	Assignment [21,30,38–40]
Magnetite	297	298	T_{2g} (Fe–O asym. bend)
	–	319	E_g (Fe–O sym. bend)
	523	540	T_{2g} (Fe–O asym. bend)
	666	668	A_{1g} (Fe–O sym. str)
Goethite	223	–	Fe–O sym. str
	297	299	Fe–OH sym. bend
	392	400	Fe–O–Fe/–OH sym. str
	484	–	Fe–OH asym. str
	564	550	Fe–OH asym. str
	674	–	Fe–O sym. str
Hematite	226	225	A_{1g} (Fe–O sym. str)
	–	247	E_g (Fe–O sym. bend)
	292	293	E_g (Fe–O sym. bend)
	406	412	E_g (Fe–O sym. bend)
	495	498	A_{1g} (Fe–O sym. str)
	600	613	E_g (Fe–O sym. bend)
	700	–	A_{1g} (Fe–O sym. str)
Maghemite	358	344	E_g (Fe–O sym. str)
	–	390	T_{2g} (Fe–O asym. bend)
	499	507	T_{2g} (Fe–O asym. bend)
	678	665	A_{1g} (sym. str)
	710	721	A_{1g} (sym. str)

Table 5
Prepared iron oxides and their corresponding particle sizes, shapes and surface area values

Compound	Shape	Size (μm)	Surface area (m^2g^{-1})
Magnetite	Pseudocubic	<0.1	90
Pure magnetite	Pseudocubic	<0.1	75
Goethite	Needle-like/acicular	<0.05	113
Pure goethite	Needle-like	<0.1	39
Maghemite	Irregular	<0.1	87
Pure maghemite	Pseudocubic	<1	20
Hematite	Pseudocubic	<0.05	~1
Pure hematite	Pseudocubic	<0.05	6.2

close as possible to the ideal one (Fe_3O_4) [28]. The magnetite stoichiometry obtained in this study is acceptably close. The correct stoichiometry ensures that there is little or no inclusion of other phases, e.g. hematite, into the synthetic magnetite to reduce the denseness of the black colour achieved.

Short time ageing resulted in a deep green precipitate, most likely green rust [8], which is expected to contain Fe^{2+}, Fe^{3+}, OH^- and SO_4^{2-} [12]. Observing the colour change from deep green to black with increase in ageing time easily followed the conversion from the green colloidal particles to spinel. The bulk of the solution was black after 5 h of ageing. However, a brown (rust colour) tinge was visible on the surface even after 8 h. This was perhaps due to the presence of an amount of unoxidized iron [27], FeOOH [25] or Fe_2O_3 detected in the ferrous precursor. By increasing the ageing time to 20 h the brown tinge disappeared and only very fine deep black colloidal particles were observed. The analysis of the product obtained after 20 h using SEM showed particles with pseudocubic shapes, Fig. 2.

This technique further showed that the product was composed of aggregates of minute particles of less than 1 μm in size. Such small particle size values indicate that the pigment will show high tinting strength [37]. The particles were regular and uniform suggesting that the pigment will show a quality hiding power [25,37]. Raman spectroscopy also confirmed the presence of magnetite (see Fig. 3, Table 4).

The surface area value of this product (90 m^2/g) is higher than that for standard products (commercial magnetite and magnetite obtained from pure starting material) as shown in Table 5. This could mean that the magnetite prepared in this study was highly porous. The surface area affects essentially the oil absorption ability of pigment such that the higher the surface area the greater is the oil absorption [37].

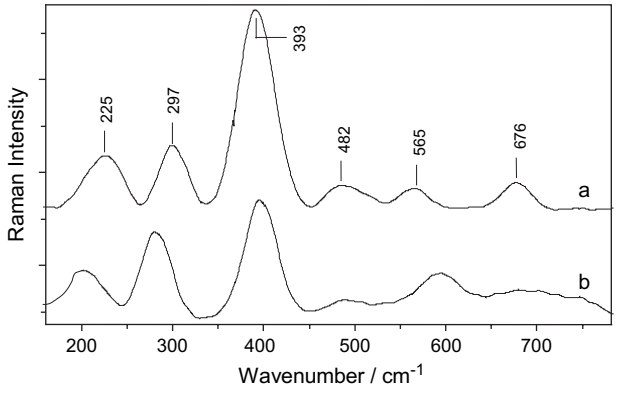

Fig. 4. Raman spectra of goethite from (a) pure starting material and (b) millscale.

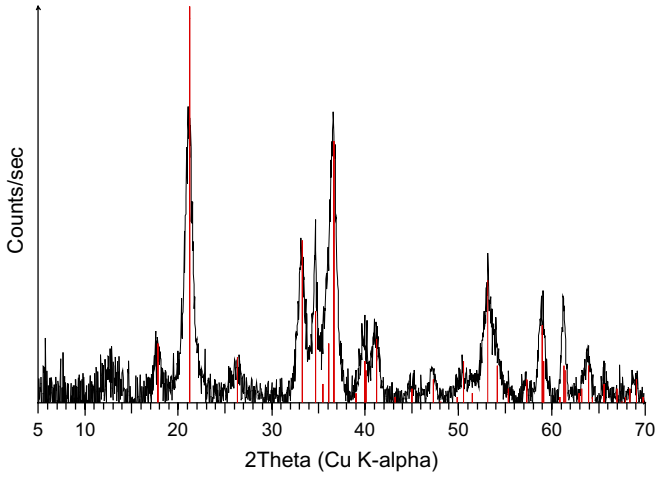

Fig. 5. X-ray powder diffractogram of goethite obtained from mill scale.

3.3. Goethite

The Raman spectroscopic analysis identified the phase of this product to be goethite, Table 4 and Fig. 4, as shown by the presence of the characteristic bands of goethite. Raman bands occurring at 223 and 674 cm^{-1} were assigned to the Fe–O A_{1g} mode and Fe–O stretching, respectively. Therefore, product showed the presence of small amounts of hematite impurity (223 cm^{-1}). The band around 483 cm^{-1} was not assigned. There is a strong possibility that the unassigned band is due to some impurities which are either amorphous or occur in small amounts only detectable by the Raman technique because of its microscopic nature. These impurities possibly interfere with the crystallinity of goethite.

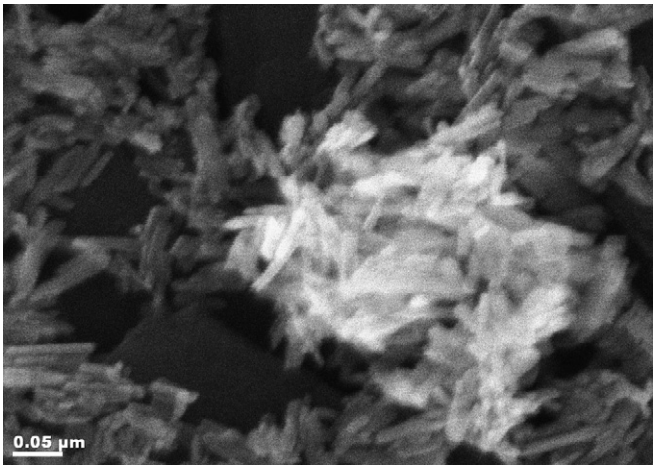

Fig. 6. SEM micrograph of goethite obtained from mill scale.

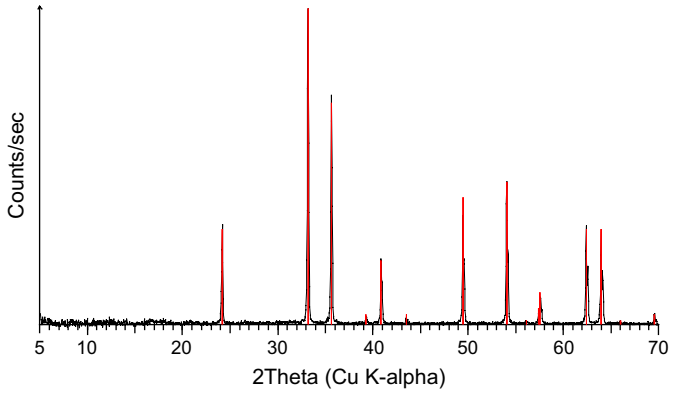

Fig. 7. X-ray powder diffractogram of hematite obtained from mill scale goethite at 750 °C.

The XRD analysis of the yellow powder showed goethite to be the main phase. The slight broadening of the XRD lines (Fig. 5) may be due to the poor crystallinity, impurities and small particle sizes. The hematite phase could not be detected by XRD analysis. The surface area value of goethite sample is far higher than that of the standard product (Table 5).

The SEM micrograph of goethite product (Fig. 6) showed that the particle size was less than 0.05 μm, a sign of high tinting strength [24]. The particles from bright yellow goethite were needle-like in shape and fairly regular. This indicates the quality hiding power that the pigment will show [25].

3.4. Hematite

The calcination of mill scale-derived goethite resulted in hematite phase as detected by X-ray diffraction. From the XRD lines (Fig. 7) it can be said that the product is fairly crystalline. This product seems to be relatively pure.

The Raman spectra also showed the presence of hematite characteristic bands in the region 200–700 cm^{-1} (Fig. 8, Table 4). Different shades of red colour were obtained, when thermal decomposition was carried out at different temperatures, including brownish-orange (650 °C for 3 h), brownish-red (700 °C for 5 h), bright-red (750 °C for 3 h), maroon/purple (800 °C for 5 h) and gray (900 °C for 5 h).

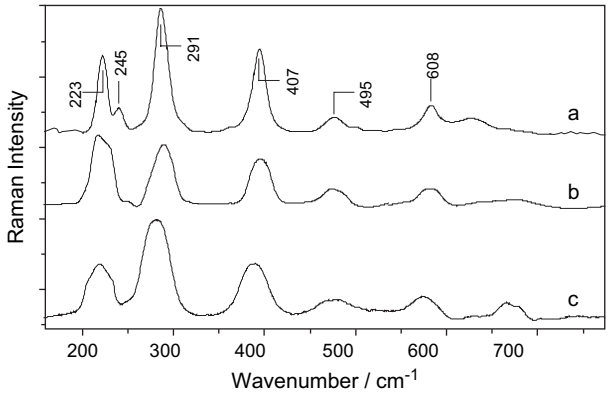

Fig. 8. Raman spectra of hematite from various sources: (a) commercial hematite; (b) hematite from pure starting material and (c) hematite from mill scale.

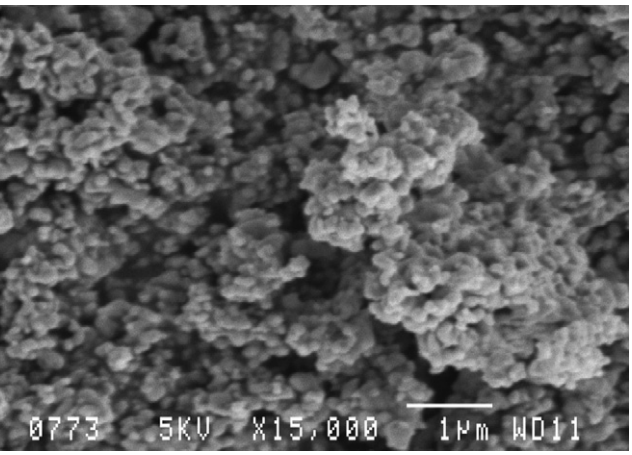

Fig. 9. SEM micrograph of hematite obtained from mill scale goethite at 750 °C.

SEM results of the product obtained at 750 °C showed very small particle sizes and uniform pseudocubic shapes (Fig. 9, Table 5). The hematite particles obtained at 750 °C were fairly regular and have surface area value comparable with that of the commercial product. Therefore, this pigment will show high tinting strength, good oil absorption ability and hiding power [24,25,37].

3.5. Maghemite

This product was identified by its broad Raman characteristic features around 358, 499 and 710 cm^{-1} (Table 4, Fig. 10) [38–40]. The XRD analysis (Fig. 11) also confirmed the presence of maghemite, even though not fully crystalline. The broad feature around 2θ value of 13 (Fig. 11) is due to the instrumental drift. The product may contain some small quantity of impurities (most likely magnetite and hematite). The surface area values are higher than those of the standard products. The particles were irregular and showed sizes below 1 μm (Fig. 12). Pigments with particle sizes below 10 μm

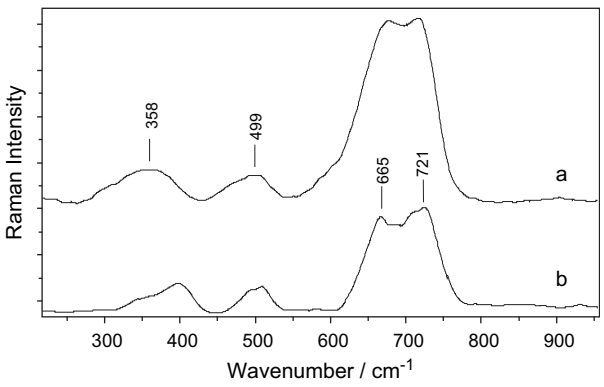

Fig. 10. Raman spectra of maghemite from (a) pure starting material and (b) mill scale.

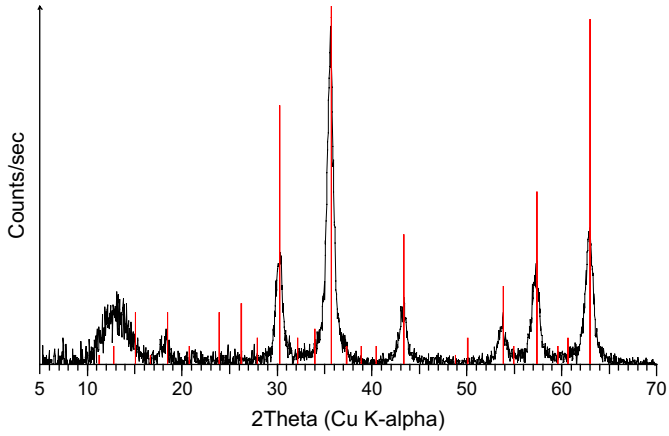

Fig. 11. X-ray powder diffractogram of maghemite obtained from mill scale magnetite at 200 °C.

normally show good pigment properties [28], including high tinting strength and oil absorption [24,25,37].

4. Conclusion

This study has shown that it is possible to prepare magnetite (black), hematite (red), goethite (yellow) and maghemite (brown) pigments of acceptable purity and with good morphological properties (i.e. particle size, shape, colour and surface area) from mill scale iron waste through simple and cost effective methods. The formation of iron oxide precursors (sulphate-containing compounds with iron as Fe^{2+} in one case and Fe^{3+} in another) has facilitated the precipitation of both magnetite and goethite in an aqueous medium. This has also led to the precipitation of pigments with particle sizes below 0.1 μm. The advantages of such small particle sizes are manifested by the good colour tones and intensity of magnetite (black) and goethite (yellow). Various shades of red colour were obtained depending on the temperature and duration of calcination of goethite. The thermal treatment of the obtained magnetite at 200 °C for 3 h resulted in maghemite. Generally, high surface area values obtained for all iron oxides prepared in this study when compared with standard products suggest that the pigments were highly porous. Due to the small particle sizes (<0.1 μm) of the iron oxides under study, the pigments prepared in this way will show good tinting strength, hiding powder and oil absorption.

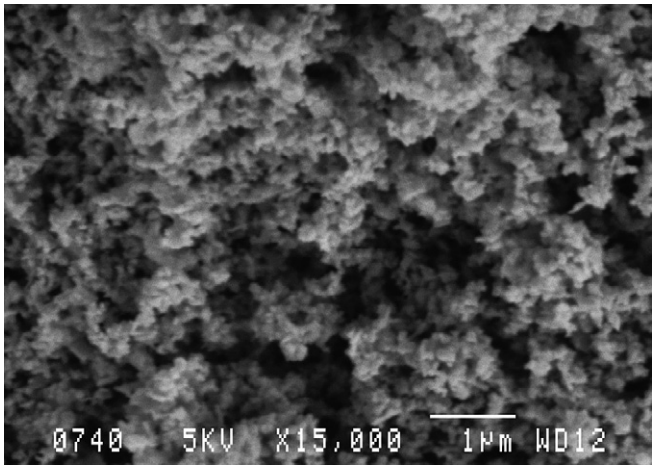

Fig. 12. SEM micrograph of maghemite obtained from mill scale magnetite at 200 °C.

Acknowledgement

The financial support by the National Research Foundation in Pretoria and the University of Pretoria is gratefully acknowledged. The authors thank the MITTAL STEEL, Pretoria, for the supply of mill scale iron waste.

References

[1] Lopez-Delgado A, Peña C, López V, López FA. Resour Conserv Recycl 2003;40:39–51 and references therein.
[2] International Iron and Steel Institute. The management of steel industry by-products and waste. Brussels Committee on Environmental Affairs; 1987.
[3] International Iron and Steel Institute. The management of plant ferruginous by-products. Brussels Committee on Environmental Affairs and Committee on Technology; 1994.
[4] Reference document on best available techniques in the ferrous metals processing industries. Spain: IPPC Directive European Commission, Institute for Prospective Technological Studies Seville, Directorate-General Joint Research Centre; October 2000.
[5] Solć Z, Trojan M, Brandova D, Kuchler M. J Therm Anal 1988;33:463–9.
[6] Allen RLM. Color chemistry. London: Thomas Nelson and Sons Ltd; 1971. p. 87.
[7] Sugimoto T, Muramatsu A, Sakata K, Shindo D. J Colloid Interface Sci 1993;158:420–8.
[8] Ueda M, Shimada S, Inaga M. J Eur Ceram Soc 1996;16:685–6 and references therein.
[9] Tamaura Y, Ito K, Katsura T. J Chem Soc Dalton Trans 1983;1983:189–94.
[10] Bate G. In: Wohlfarth EP, editor. Ferromagnetic materials, vol. II. North-Holland; 1980. p. 406.
[11] Leskelä T, Leskelä M, Niinisto L. Thermochim Acta 1984;72:229–37.
[12] Ismail HM, Gadenhead DA, Zaki MI. J Colloid Interface Sci 1996;183:320–8.
[13] Ismail HM, Zaki MI, Hussein GA, Magar MN. Powder Technol 1990;63:87–96.
[14] Bailey JK, Brinker CJ, Mecartney ML. J Colloid Interface Sci 1993;157:1–13.
[15] Itoh H, Sugimoto T. J Colloid Interface Sci 2003;265:283–95.
[16] Rao V, Sashimohan AL, Biswas AB. J Mater Sci 1974;9:430–3.
[17] Ravindranathan P, Patil KC. J Mater Sci Lett 1986;5:221–2.
[18] Narasimhan BRV, Prabhakar S, Manohar P, Gnanam FD. Mater Lett 2002;52:295–300 and references therein.
[19] Luo H, Zeng H. J Therm Anal 1995;45:185–91.
[20] Nunez NO, Morales MP, Tatraj P, Serna CJ. J Mater Chem 2000;10:2561–5.
[21] Nauer G, Strecha P, Brinda-Konopik N, Liptay G. J Therm Anal 1985;30:813–25 and references therein.
[22] Kalinskaya TV, Krasotkin IS, Lobanova LB. J Appl Chem USSR 1979;520:955–8.
[23] Thiebeau RJ, Brown CW, Heidersback RH. Appl Spectrosc 1978;32:532–5 and references therein.
[24] Ismail HM, Fouad NE, Zaki MI, Magar MN. Powder Technol 1992;70:183–8.
[25] Fouad NE, Ismail HM, Zaki MI. J Mater Sci Lett 1998;17:27–9.

[26] Škvara F, Kaštanek F, Pavelkova I, Šolcova O, Maleterova Y, Scheider P. J Hazard Mater 2002;89:67–81.
[27] Coburn SK, editor. Corrosion source book. Metals Park, OH: American Society For Metals; 1984. p. 12–3.
[28] Oulsnam BT, Erasmus D. US Patent 5,738,717,1998.
[29] Li Yuang-Shen. Waste Manag 1999;19:495–502.
[30] de Faria DLA, Silva SV, de Oliviera MT. J Raman Spectrosc 1997;28:873–8 and references therein.
[31] Labspec, version 2.04, Distributed by Dilor SA & Universite' de Reims, France; 1997.
[32] Verryn S. Details of XRD procedure used at the University of Pretoria XRD laboratory, personal written communication, University of Pretoria, Pretoria; 2002.
[33] Loubser ML. (Typed) Report on XRF analyses of ceramics, mloubser@postino.up.ac.za; 20 June 2002.
[34] Bennet H, Oliver G. XRF analysis of ceramics, minerals and applied materials. Chichester: Wiley; 1997. p. 37.
[35] Watson JS. X-ray spectrom 1996;25:173–4.
[36] Musić S, Orehovec Z, Popović S, Czakó-Nagy I. J Mater Sci 1994;29:1991–8.
[37] Turner GPA. Introduction to paint chemistry and principles of paint technology. 2nd ed. London: Chapman and Hall; 1980. p. 95–107.
[38] Dunnwald J, Otto A. Corros Sci 1989;29:1167–76.
[39] Kieser JT, Brown CW, Heidersbach RH. Corros Sci 1983;23:251–9.
[40] Boucherit N, Hugot-Le Goff A, Joiret S. Corros Sci 1991;32:497–507.